Photoinduced Opposite Diffusion of Nematic and Isotropic Monomers during Patterned Photopolymerization

Cornelus F. van Nostrum† and Roeland J. M. Nolte

Department of Organic Chemistry, N.S.R. Center, University of Nijmegen, Toernooiveld, 6525 ED Nijmegen, The Netherlands

Dirk J. Broer*

Philips Research Laboratories, Prof. Holstlaan 4, 5656 AA Eindhoven, The Netherlands

Thomas Fuhrman and Joachim H. Wendorff

Department of Physical Chemistry, Philipps-Universität Marburg, 35032 Marburg, Germany

Received May 2, 1997. Revised Manuscript Received November 4, 1997[⊗]

Films containing a photoreactive mixture of a liquid-crystalline diacrylate and an isotropic monoacrylate were UV exposed by means of lithographic and holographic techniques, resulting in a spatial intensity distribution in the films. The favored depletion of the more reactive diacrylate at sites with maximum UV intensity results in preferred diffusion of this monomer to these areas. The monoacrylate oppositely diffuses to the sites with minimum intensity which, depending on polymer ratios and liquid-crystalline transition temperatures, eventually leads to a phase transition from the nematic to the isotropic phase. In this way holographic gratings were prepared exhibiting high diffraction efficiencies due to the alternation of lines of optically oriented and of isotropic materials. The diffusion process was successfully simulated by a simple polymerization and diffusion model and was verified by fluorescent labeling experiments in combination with fluorescence microscopy.

Introduction

Materials with spatial variations of properties and composition are receiving increased interest as they may be applied in data storage systems and in optical devices. Changes that may be locally induced by varying the composition of the material are the refractive index, the phase (e.g., isotropic or liquid crystalline), or the chirality. Light is a convenient tool for the creation of patterned changes, e.g., by inducing photoisomerization, photodissociation, or photopolymerization reactions. An example is the helical pitch gradient which can be created in a cholesteric polymer network by exposing a photopolymerizable cholesteric liquid-crystalline mixture to a UV intensity gradient.[1] The resulting films behave as a broad-band reflective polarizer.

Spatial modulation of the refractive index may be used for the construction of so-called volume phase holograms by illuminating commercially available films using an interference pattern. The well-known DuPont photopolymer film[2] is a mixture of polymeric binder, a monomer, and a photoinitiator. Exposure of this film to a fringe pattern causes depletion of the monomer in the regions with high light intensities, and as a result diffusion of monomer from the dark to the light regions occurs.[3−6] After fixation of the hologram, which is accomplished by uniform exposure, the light fringes have a higher concentration of polymer than the dark ones. The resulting thickness and refractive index variations in the material are responsible for the diffracting properties of the gratings.

More recently, Sutherland and Bunning described the use of polymer-dispersed liquid-crystal (PDLC) formulations for holographic recording.[7−10] During the polymerization of mixtures of a monomer and a liquid-crystalline (LC) compound, the unreactive LC molecules diffuse to the dark fringes of the applied pattern, giving rise to periodic planes enriched with LC droplets. With

† Present address: Eindhoven Polymer Laboratories, Department of Coatings Technology, Eindhoven University of Technology, P.O. Box 513, 5600 MB, Eindhoven, The Netherlands.

[⊗] Abstract published in *Advance ACS Abstracts,* December 15, 1997.

(1) Broer, D. J.; Lub, J.; Mol, G. N. *Nature* **1995**, *378*, 467.

(2) Haugh, E. F. *Hologram Recording in Photopolymerizable Layers*, U.S. Patent, 3658526, 1972, assigned to E. I. du Pont de Nemours and Co.

(3) Colburn, W. S.; Haines, K. A. *Appl. Opt.* **1971**, *10*, 1636.

(4) Wopschall, R. H.; Pampalone, T. R. *Appl. Opt.* **1972**, *11*, 2096.

(5) Rhee, U.-S.; Caulfield, H. J.; Vikram, C. S.; Shamir, J. *Appl. Opt.* **1995**, *34*, 846.

(6) Zhao, G.; Mouroulis, P. *J. Modern Opt.* **1994**, *41*, 1929.

(7) Sutherland, R. L.; Natarajan, L. V.; Tondiglia, V. P.; Bunning, T. J. *Chem. Mater.* **1993**, *5*, 1533.

(8) Tondiglia, V. P.; Natarajan, L. V.; Sutherland, R. L.; Bunning, T. J.; Adams, W. W. *Opt. Lett.* **1995**, *20*, 1325.

(9) Sutherland, R. L.; Tondiglia, V. P.; Natarajan, L. V.; Bunning, T. J.; Adams, W. W. *Appl. Phys. Lett.* **1994**, *64*, 1074.

(10) Bunning, T. J.; Natarajan, L. V.; Tondiglia, V.; Sutherland, R. L.; Vezie, D. L.; Adams, W. W. *Polymer* **1995**, *36*, 2699.

S0897-4756(97)00305-0 CCC: $15.00
Published on Web 01/01/1998

Chart 1

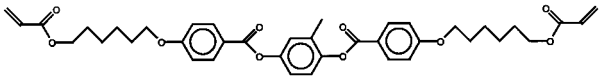

DA

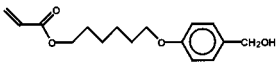

MA

these systems electrically switchable holographic gratings were constructed. Reflection holograms, which contain periodic layers parallel to the film surface, have also been described based on PDLCs.[11−14]

Sponsler et al. used the liquid-crystalline monomer **DA** shown in Chart 1 for the formation of switchable holographic gratings.[15,16] These gratings consist of alternating layers of monomer and crosslinked polymer. Switching between on and off states can be accomplished by an electric field, which will enforce the orientation of the remaining monomer to be perpendicular (large refractive index modulation) or parallel to the polymer orientation (virtually no refractive index modulation). The hologram can be fixed by postexposure with light of uniform intensity.

The diffraction efficiency of a volume hologram is related to the amplitude of the refractive index modulation.[17] Our research aims at the development of polarizing holographic gratings with high diffraction efficiencies by the in situ formation of alternating isotropic fringes having a low refractive index n_i and oriented nematic fringes. If n_i equals the low refractive index n_o of the birefringent fringes, diffraction will occur only for incident light polarized parallel to the molecular director orientation of the nematic areas. The present paper shows that such structures can be obtained by making use of diffusion processes during holographic as well as lithographic polymerization of homogeneous mixtures of an isotropic and a nematic compound with different photoreactivities. This principle has been recognized for the first time 20 years ago[18] but has not been applied for anisotropic systems.

The principle of this process is schematically shown in Figure 1. A mixture of **DA** and **MA** (Chart 1) in its nematic phase is illuminated using an interference pattern. Within the light fringes the most reactive **DA** monomer is depleted faster, inducing a concentration gradient. This initiates a diffusion process, in which **DA** molecules move to the light fringes and the isotropic component **MA** moves to the dark fringes. The enrichment of the isotropic monomer in the dark regions may

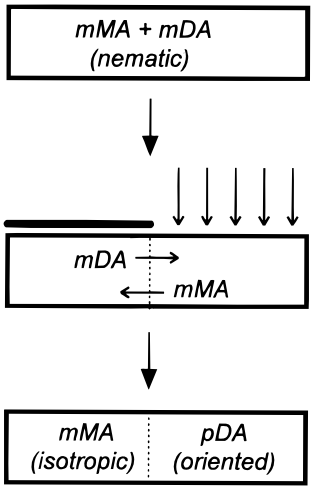

Figure 1. Schematic representation of the diffusion process that takes place when a mixture of monoacrylate (mMA) and diacrylate (mDA) monomers is locally illuminated.

enforce a phase transition from the nematic to the isotropic phase. Subsequent illumination with uniform light can fix the grating. In this paper experiments and model calculations are presented showing that the above-mentioned process is feasible.

Experimental Section

Materials. The diacrylate 2-methyl-1,4-bis[4-[6-(acryloyloxy)hexyloxy]benzoyloxy]benzene (**DA**) was supplied by Merck. Chlorohexyl acrylate was kindly donated by Dr. J. Lub from Philips Research Laboratories. The fluorescent probe 9-anthroyl nitrile was prepared as described in ref 19. Other reagents and solvents were used as supplied.

Synthesis of 6-[4-(Hydroxymethyl)phenyloxy]hexyl Acrylate (MA). 6-Chlorohexyl acrylate (10 g, 0.053 mol), NaI (8.8 g, 0.059 mol), and a small amount of 2,6-di-*tert*-butyl-4-methylphenol were refluxed in butanone (100 mL) for 5.5 h. The precipitate was filtered off, and 4-(hydroxymethyl)phenol (7.2 g, 0.058 mol) and K_2CO_3 (10 g, 0.072 mol) were added to the solution. After this was refluxed for 40 h, the precipitate was filtered off and the solvent was evaporated. The product was dissolved in diethyl ether, washed with aqueous 10% NaOH and with water, and dried over $MgSO_4$. The monoacrylate was purified further by column chromatography on silicagel (60H) using 2% ethyl acetate in dichloroethane as the eluent. *p*-Methoxyphenol (100 ppm) was added as an inhibitor (to prevent premature polymerization). Yield: 8.5 g (58%) of a clear viscous oil. ^{1}H NMR ($CDCl_3$) δ 1.4−1.85 (m, 8H, CH_2), 3.97 (t, 2H, CH_2OAr), 4.18 (t, 2H, CH_2OAcr), 4.62 (s, 2H, OCH_2-Ar), 5.81−6.39 (m, 3H, $CH{=}CH_2$), 6.88 (d, 4H, Ar).

Measurements. Differential scanning calorimetry (DSC) was carried out with a Perkin-Elmer DSC 7 instrument. For photo-DSC, samples containing 100 ppm *p*-methoxyphenol and 1 wt % of photoinitiator (Irgacure 184, Ciba-Geigy) were illuminated with a Philips PL S-9W/10 lamp (0.8 mW cm^{-2}, 360 nm) at constant temperature.

Refractive indexes were measured with a Carl Zeiss or an Atago thermostated refractometer. Polarizing microscopy (PM) was performed with a Leitz Orthoplan and a Leitz Aristomet microscope. The birefringence of the samples was measured with a Leitz tilting compensator K. Scanning electron microscopy (SEM) micrographs were obtained with a Philips SEM 525M instrument, after removal of the cover substrate and coating with a thin layer of gold. Surface profiles were measured with a Tencor Instruments Alpha-step 200 Surface Profiler. Atomic force microscopy (AFM) was

(11) Tanaka, K.; Kato, K.; Tsuru, S.; Sakai, S. *Conf. Proc. 13th Int. Display Res. Conf.* **1993**, 109.
(12) Tanaka, K.; Kato, K.; Date, M.; Sakai, S. *Conf. Proc. SID 95 DIGEST*, 267.
(13) Date, M.; Naito, N.; Tanaka, K.; Kato, K.; Sakai, S. *Conf. Proc. Asia Display '95*, 603.
(14) Bunning, T. J.; Natarajan, L. V.; Tondiglia, V. P.; Sutherland, R. L.; Vezie, D. L.; Adams, W. W. *Polymer* **1996**, *37*, 3147.
(15) Zhang, J.; Carlen, C. R.; Palmer, S.; Sponsler, M. B. *J. Am. Chem. Soc.* **1994**, *116*, 7055.
(16) Sponsler, M. B. *J. Phys. Chem.* **1995**, *99*, 9430.
(17) Kogelnik, H. *Bell Syst. Tech. J.* **1969**, *48*, 2909.
(18) Tomlinson, W. J.; Chandross, E. A.; Weber, H. P.; Aumiller, G. D. *Appl. Opt.* **1976**, *15*, 534.
(19) Goto, J.; Goto, N.; Shamsa, F.; Saito, M.; Komatsu, S.; Suzaki, K.; Nambara, T. *Anal. Chim. Acta* **1983**, *147*, 397.

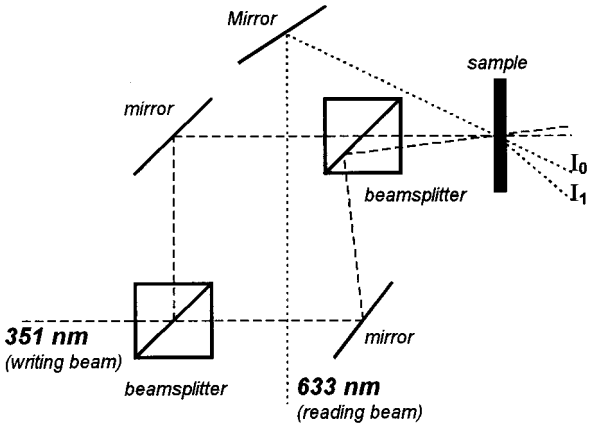

Figure 2. Experimental setup for the holographic recording and simultaneous reading. The intensities of the zero-order undiffracted reading beam (I_0) and the first-order diffracted beam (I_1) are measured with photodetectors.

carried out with a Topometrix TMX 2000 instrument and optical microscopy with an Olympus BX60 microscope. Fluorescence spectra were obtained with a Perkin-Elmer LS50 luminescence spectrometer (λ_{ex} = 370 nm). Fluorescence microscopy was carried out with a Leitz Laborlux D microscope equipped with a Philips CCD camera. Fluorescence images were digitized with the help of the PCgrab-G1/G2 framegrabber from Matrix Vision and analyzed with the Image-Pro Plus program.

Sample Preparation. Glass slides (1 mm thick) were cleaned by subsequently washing with a detergent solution, demineralized water, and 2-propanol and were treated with UV/ozone for 10 min. A thin layer of polyimide precursor (AL1051 supplied by JSR) was applied by spin-coating and cured in vacuum at 170 °C for 1 h. Orientation of the polyimide was realized by rubbing with a nylon cloth. One glass slide was spin-coated with a suspension of 6 μm silica spheres in ethanol, and a second slide was adhered with the rubbing directions being parallel. The obtained cells were filled by capillary suction with mixtures containing **MA**, **DA**, 100 ppm inhibitor (*p*-methoxyphenol), and 1 wt % photoinitiator (Irgacure 184), in the melt.

Lithography. A grating mask composed of parallel lines of chrome with grating constants varying from 10 to 1000 μm was positioned on top of a filled sample cell. The cells were illuminated for 15 min at various temperatures with a collimated UV beam (320 nm, 0.3 mW cm^{-2}) using a Karl Süss MJB3 contact illuminator. After this period, the cells were illuminated for 1 min without the grating mask using an intensity of 3 mW cm^{-2}.

Holography. Holographic gratings were obtained by using the Mach−Zehnder interferometer setup shown in Figure 2. An Ar laser beam (351 nm, beam diameter ca. 1.5 mm) was separated into two beams of equal intensity (typically 1.2 mW cm^{-2}) by a beam splitter and recombined by using a second beam splitter. The angle between the recombined beams was adjusted to obtain a grating constant of 10 μm. Samples similar as used for the lithographic experiments, with varying **MA**/**DA** ratios, were illuminated at various temperatures. During holographic recording, the diffraction efficiencies of the gratings were measured simultaneously with a 633 nm He−Ne laser beam. The diffraction efficiency (η) was calculated from the intensity of the transmitted beam (I_0) at the start of the grating formation and the intensity of the first order diffracted beam (I_1) at time t according to

$$\eta(t) = I_1(t)/I_0(0) \tag{1}$$

After recording, the films were illuminated with a single laser beam to fix the hologram.

Fluorescent Labeling. One of the two glass slides of each cell containing a polymerized film was removed, and the samples were placed for 16 h at room temperature in a bath containing 25 mg of 9-anthroylnitrile, 1.2 mg of 4-(dimethylamino)pyridine, and 150 mL of dry acetonitrile. Subsequently the films were thoroughly rinsed with methanol and acetonitrile.

Calculations. A one-dimensional model was applied to simulate the diffusion processes that occur during the nonuniform polymerization of a mixture of two compounds with different reactivities. The total area was partitioned into n positions, and in each position small polymerization steps were alternated with diffusion steps in which complete diffusion over the whole area to an equilibrium situation was supposed. The molar fractions of the two monomeric acrylates, [mMA] and [mDA], and the molar fractions of the acrylates that have been incorporated in the polymer, [pMA] and [pDA], were calculated after each polymerization step t at position x in the film as follows:

$$[\mathrm{mMA}]_{t,x} = [\mathrm{mMA}]_{t-1,x} - I_x \times R_{\mathrm{MA}} \times [\mathrm{mMA}]_{t-1,x} \tag{2a}$$

$$[\mathrm{mDA}]_{t,x} = [\mathrm{mDA}]_{t-1,x} - I_x \times R_{\mathrm{DA}} \times [\mathrm{mDA}]_{t-1,x} \tag{2b}$$

$$[\mathrm{pMA}]_{t,x} = [\mathrm{pMA}]_{t-1,x} + I_x \times R_{\mathrm{MA}} \times [\mathrm{mMA}]_{t-1,x} \tag{2c}$$

$$[\mathrm{pDA}]_{t,x} = [\mathrm{pDA}]_{t-1,x} + I_x \times R_{\mathrm{DA}} \times [\mathrm{mDA}]_{t-1,x} \tag{2d}$$

where $[\mathrm{mMA}]_{t-1,x}$ etc. are the fractions of acrylates present before the polymerization step in each position, I_x is the relative light intensity at position x,[20] and R_{MA} and R_{DA} are the fractions of present monomers that react in each step (typically values of 0.02 and 0.04 were chosen for the monoacrylate and diacrylate, respectively, accounting for the fact that the reaction probability of a diacrylate molecule is twice as large as that of the monoacrylate).

We assumed that only free monomer is able to diffuse, which will eventually lead to equal monomer ratios in all positions. The ratio between the two monomers in each position, $r(t,x)$, after a polymerization step is described by eqs 3 and 4:

$$\phi_{\mathrm{mMA}}(t,x) = \frac{[\mathrm{mMA}]_{t,x}}{[\mathrm{mMA}]_{t,x} + [\mathrm{mDA}]_{t,x}} \tag{3a}$$

$$\phi_{\mathrm{mDA}}(t,x) = \frac{[\mathrm{mDA}]_{t,x}}{[\mathrm{mMA}]_{t,x} + [\mathrm{mDA}]_{t,x}} \tag{3b}$$

$$r(t,x) = \frac{[\mathrm{mMA}]_{t,x}}{[\mathrm{mDA}]_{t,x}} = \frac{\phi_{\mathrm{mMA}}(t,x)}{\phi_{\mathrm{mDA}}(t,x)} \tag{4}$$

Each infinitely long diffusion step can best be described by taking together all the monomers, and mixing and redistributing them over all the positions. Mathematically this can be expressed as follows: First, all monomers are taken together:

$$\sum mMA = \sum_{x=1}^{n} [\mathrm{mMA}]_{t,x} \tag{5a}$$

$$\sum mDA = \sum_{x=1}^{n} [\mathrm{mDA}]_{t,x} \tag{5b}$$

The monomer fractions Φ of the monoacrylate and the diacrylate in this virtual mixture are then

(20) The polymerization rate is proportional to I_x^a, in which the exponent a depends on the termination mechanism of the free-radical chain polymerization. The value of a is 0.5 in the case of a bimolecular termination reaction and 1 in the case of a termination reaction by a monomolecular radical trapping reaction. It has been reported that for photoinitiated polymerization of diacrylates $a = 0.7$ at the reaction onset and that this value approaches 1 as the reaction proceeds and the living chain ends are prevented to reach each other. For reasons of simplicity we have taken a to be equal to 1. See ref 23 and: Kloosterboer, J. G.; Lijten, G. F. C. M.; Zegers, C. P. G. *PMSE* **1989**, *60*, 122.

$$\Phi_{\mathrm{mMA}} = \frac{\sum mMA}{\sum mMA + \sum mDA} \quad (6a)$$

$$\Phi_{\mathrm{mDA}} = \frac{\sum mDA}{\sum mMA + \sum mDA} \quad (6b)$$

The mixture has to be redistributed over the positions. The new monomer fractions in each position $\phi_{\mathrm{mMA}}(t+1,x)$ and $\phi_{\mathrm{mDA}}(t+1,x)$ should be equal to Φ_{mMA} and Φ_{mDA}, respectively (which then gives equal monomer ratios $r(t+1,x)$ for all positions after redistribution). Besides, in every position the total amount of monomer after diffusion ($[\mathrm{mMA}]_{t+1,x} + [\mathrm{mDA}]_{t+1,x}$) should be equal to that before diffusion ($[\mathrm{mMA}]_{t,x} + [\mathrm{mDA}]_{t,x}$). According to these conditions, the new values of the mole fractions that are used for the next polymerization step (eq 2a−d) can be calculated as follows:

$$[\mathrm{mMA}]_{t+1,x} = \Phi_{\mathrm{mMA}} \times ([\mathrm{mMA}]_{t,x} + [\mathrm{mDA}]_{t,x}) \quad (7a)$$

$$[\mathrm{mDA}]_{t+1,x} = \Phi_{\mathrm{mDA}} \times ([\mathrm{mMA}]_{t,x} + [\mathrm{mDA}]_{t,x}) \quad (7b)$$

$$[\mathrm{pMA}]_{t+1,x} = [\mathrm{pMA}]_{t,x} \quad (7c)$$

$$[\mathrm{pDA}]_{t+1,x} = [\mathrm{pDA}]_{t,x} \quad (7d)$$

It should be noted that in the procedure described above any possible difference in molar volume between the monoacrylate and the diacrylate is not taken into account and that the described situation is valid only when the diffusion rate is high as compared to the polymerization rate.

Results and Discussion

Monomers and Mesomorphic Properties. For our experiments we used mixtures of the two compounds shown in Chart 1. The diacrylate **DA** is a well-known compound, which displays a nematic phase between 86 and 116 °C.[21] The novel monoacrylate **MA** was synthesized as described in the Experimental Section. This monoacrylate has the advantageous properties that it is isotropic at room temperature but not volatile at elevated temperatures, it is miscible with the diacrylate, and it contains a reactive alcohol function that we used for detection purposes.

On heating freshly prepared mixtures of **MA** and **DA**, a transition from the crystalline to the nematic phase (below ca. 30 mol % **MA**) or to the isotropic phase (above ca. 30 mol % **MA**) was observed (Figure 3). On subsequent cooling, all mixtures gave a nematic phase, which crystallized slowly at room temperature. The nematic to isotropic phase transition temperatures are plotted in Figure 3 for mixtures consisting of different **MA**/**DA** ratios.

Polymerization Kinetics. Photopolymerization was recorded by measuring the heat of polymerization in a photo-DSC apparatus. Figure 4 displays the heat flow for mixtures containing different **MA**/**DA** ratios at 60 °C. It is clear from this figure that the polymerization rate of **MA** is much lower than that of **DA**. This is understandable because the number of acrylate groups in **MA** is half that in **DA**, but the major cause probably is the autoacceleration or Trommsdorf effect, which is much more pronounced for **DA** than for **MA** since gelation due to network formation occurs early in the

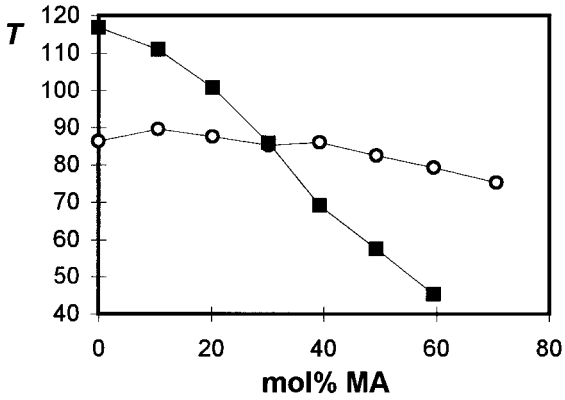

Figure 3. Melting temperatures (○) and clearing temperatures (■) of mixtures containing different molar ratios of **MA**/**DA** (the data for the clearing temperatures were obtained from a second heating run before crystallization could take place; see text).

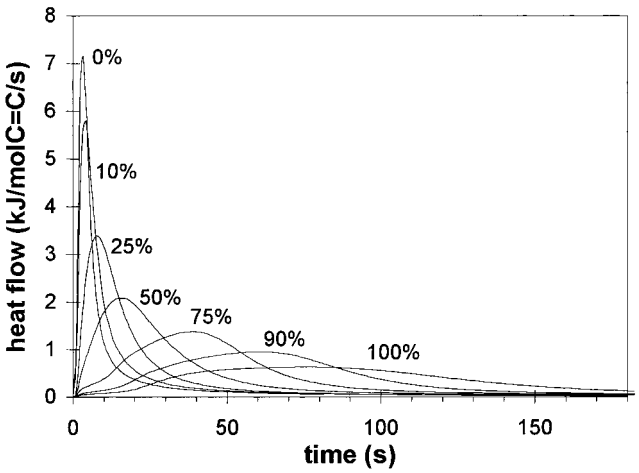

Figure 4. Isothermal DSC curves for the photopolymerization of mixtures containing various mol % **MA** at 60 °C.

polymerization of **DA** and not in the polymerization of **MA**. To exclude the possibility that the benzylic alcohol function in **MA** causes the observed effect, viz. by inhibiting the reaction, we also polymerized **DA** in the presence of the saturated analogue of **MA** (propionate instead of acrylate), but this compound did not influence the polymerization rate of **DA**.

The polymerization rates of LC diacrylates are known to be temperature dependent, and normally no discontinuity is seen at the nematic-to-isotropic phase transition.[22] For pure **DA** a maximum polymerization rate is found at around 100 °C.[22] We observed the maximum at 80 °C for 25 mol % **MA** and at 60 °C for 75 mol % **MA**. The polymerization rates are also dependent on the applied UV intensity.[23]

Lithographic Illumination. Thin-film samples of various **MA**/**DA** mixtures were illuminated through a photomask. The photomask contained eight different gratings with 5−500 μm wide lines separated by the same distances.

The most interesting results were obtained from films that were irradiated starting in the isotropic phase.

(21) Broer, D. J.; Hikmet, R. A. M.; Challa, G. *Makromol. Chem.* **1989**, *190*, 3201.

(22) Broer, D. J.; Mol, G. N.; Challa, G. *Makromol. Chem.* **1991**, *192*, 59.

(23) Doornkamp, A. T.; Alberda van Ekenstein, G. O. R.; Tan, Y. Y. *Polymer* **1992**, *33*, 2863.

Several remarkable features were observed by inspection of the resulting films under a light microscope with the samples placed between crossed polarizers. The edges of the 500 μm wide illuminated bands had become slightly oriented during illumination ($\Delta n \approx 0.01$), while the intermediary masked bands occasionally showed cracks and branched structures whose origin will be explained later. With 100 and 200 μm grating periodicities the illuminated and partly also the masked areas were composed of a number of parallel bright (i.e., oriented) lines with $\Delta n \approx 0.01$. Also gratings smaller than 100 μm showed striped structures that did not coincide with the photomask periodicity.

The observed multistripe patterns can be explained by diffraction phenomena at the photomask. The number of stripes and the distances between them corresponded surprisingly well with intensity maxima that we calculated with the Fresnel diffraction theory.[24] The intensity I at each point p on a screen at a distance of r from a single slit can be calculated by eq 8:

$$I(p) = 0.5 \times \{[E(u_2) - E(u_1)]^2 + [F(u_2) - F(u_1)]^2\} \quad (8)$$

where $E(u)$ and $F(u)$ are the so-called Fresnel integrals[25] and

$$u_{1,2} = y_{1,2}\sqrt{(2/\lambda r)} \quad (9)$$

with $y_{1,2}$ being the distances from p to the projection of both edges of the slit on the screen (see Figure 5a). The diffraction pattern of a multislit grating includes the summation of intensities arising from neighboring slits. The calculated result from a 50 μm period mask is shown as an example in Figure 5b and contains a repetition of one broad band and two bands with a lower intensity. A similar repetition is also seen in the corresponding micrograph (upper left area in Figure 5c).

From the experiments discussed so far, we may conclude that at local intensity maxima the polymers become oriented when illuminated from the isotropic phase. By compensating the optical retardation in the polarizing microscope with a tilting compensator with known optical axis, it was deduced that the molecular director was perpendicular to the grating lines. The values of the birefringence were low (of the order of magnitude of 0.01) and were independent of the presence or absence of the polyimide layer, rubbing direction, and UV intensity. We believe that the polymerization-induced orientation originates from unidirectional monomer flow and/or stresses built up by anisotropic volume and density changes during the polymerization process.[26,27]

The polymer films were also examined by scanning electron microscopy (SEM). The cracks and branched structures that were occasionally observed in the masked areas with the polarizing microscope appeared to be

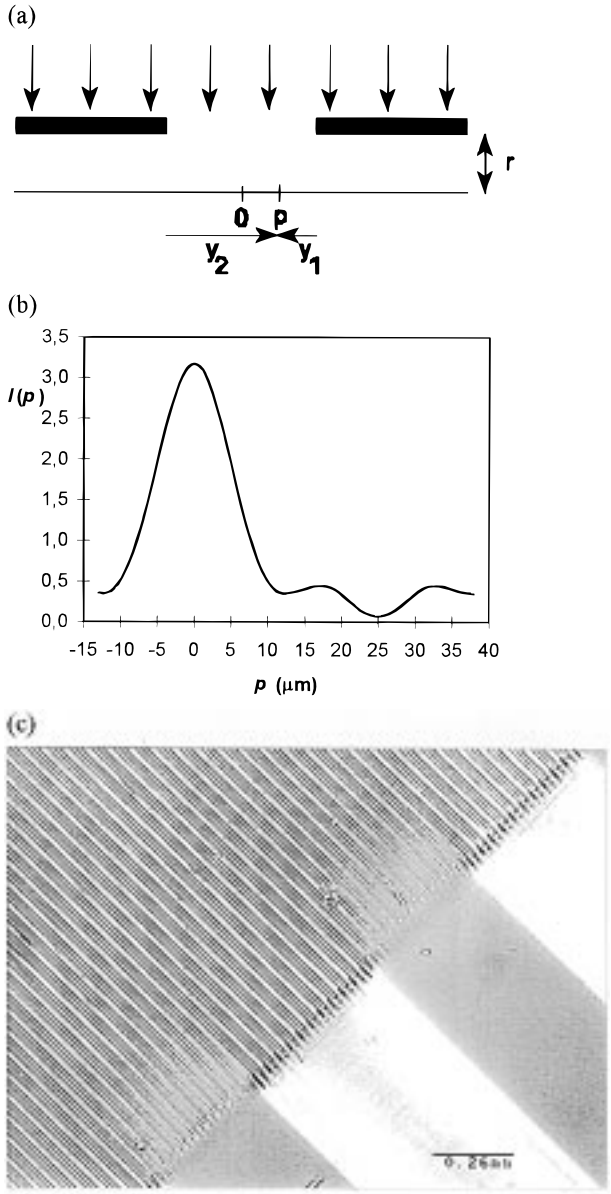

Figure 5. Fresnel diffraction during lithographic illumination: (a) explanation of the symbols used for the calculations, see text; (b) one period of the calculated intensity profile at a distance $r = 1$ mm from the photomask with a grating constant of 50 μm (λ = 320 nm); (c) polarizing micrograph (crossed polarizers) of a sample containing 50 mol % **MA** illuminated at 75 °C with a pulsed light source through a 50 μm grating (upper left area) and a 1000 μm grating (lower right area).

empty "channels". This was confirmed by surface profile measurements, which also clearly revealed that the illuminated 500 μm wide bands were ca. 3% thicker than the shadow bands (Figure 6). We believe that these thickness variations originate from the fact that we removed the upper glass plates, causing relaxation of the illuminated higher density areas. Apparently, monomer transport from the dark to the light areas causes swelling of the already formed polymer, despite the presence of the two glass boundaries. With smaller grating constants such surface profiles could not be detected by SEM but were sometimes observed with surface profile measurements, although the thickness variations were only minor (less than 100 nm).

Similar SEM and surface profile measurements were carried out on films that had been lithographically

(24) Born, M.; Wolf, E. *Principles of Optics: Electromagnetic Theory of Propagation, Interference and Diffraction of Light*, 6th ed.; Pergamon: London, 1980; section 8.7.
(25) Wijngaarden, A. V.; Scheen, W. L. *Table of Fresnel Integrals*; North Holland: Amsterdam, 1949.
(26) Krongauz, V. V.; Schmelzer, E. R. *SPIE* **1991**, *1559*, 354.
(27) Krongauz, V. V. In *Processes in Photoreactive Polymers*; Krongauz, V. V., Trifunac, A. D., Eds.; Chapman and Hall: New York, 1995; pp 185−259.

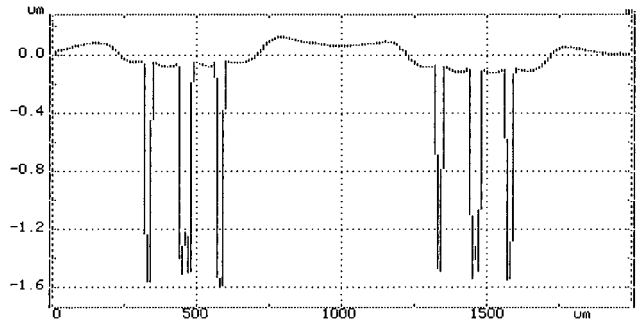

Figure 6. Surface profile of a sample containing 50 mol % **MA**, lithographically illuminated with a 1000 μm grating at 75 °C. The six narrow dips are cracks that appeared in the samples.

exposed and then, without a subsequent fixating illumination, after removal of the cover substrate, were washed with warm acetonitrile in order to extract residual monomer. From these experiments we could deduce that the films were also considerably polymerized in the masked regions, which can be explained by the aforementioned diffraction of the light at the photomask. This phenomenon will severely affect the performance of the gratings. The diffraction problems can be diminished by decreasing the distance between the mask and the film or by applying holographic exposure. The latter will be the subject of the next sections.

From the above-described experiments it can be inferred that monomer flow to the areas with maximum light intensity occurs during the lithographic illumination. It cannot be concluded yet whether this is a preferred flow of **DA** to the illuminated areas as we proposed in the Introduction. For this reason we carried out fluorescent labeling experiments on the lithographic samples, which will be described in a later section of this paper.

Another set of samples were illuminated starting in the nematic phase, which was macroscopically oriented perpendicular to the grating lines by the rubbed polyimide alignment layer on the glass substrates. After irradiation, we observed a difference in the optical retardation of the illuminated bands with respect to that of the masked bands, the illuminated bands displaying the largest retardation.

Samples that were polymerized in the biphasic phase near the phase transition temperature of the monomer mixture gave inhomogeneous films.

Holographic Recording. *Diffraction Efficiency.* The method of hologram formation and simultaneous recording of the diffraction efficiencies (η, see eq 1) of the holographic gratings is described in the Experimental Section. Holograms with a grating constant of 10 μm were recorded in thin-film samples of different **MA**/**DA** ratios at different temperatures. Figure 7a displays typical growth curves of the diffraction efficiency of samples containing 30 mol % **MA** at three different polymerization temperatures. These curves show a peak at the start of each experiment, whose origin is unknown at present. After a recording time of ca. 1 min a constant η was measured, its value depending on the temperature at which the hologram was recorded. Figure 7b shows the recording temperature dependence of the final diffraction efficiency after 5 min exposure

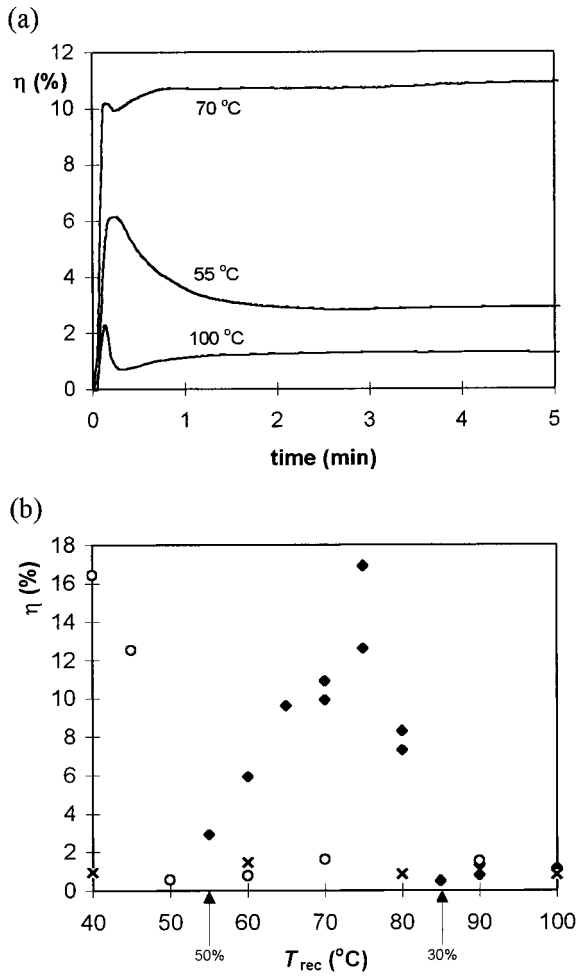

Figure 7. Diffraction efficiencies of the holograms: (a) growth of the diffraction at various recording temperatures as a function of the recording time for samples containing 30 mol % **MA**; (b) final diffraction efficiencies as a function of recording temperature for mixtures containing 30 (♦), 50 (○), and 70 (×) mol % **MA**. Arrows indicate the phase transition temperatures of the monomeric mixtures.

for three different monomer ratios. All holograms that were recorded starting in the isotropic phase gave the same low values of η (ca. 1%). Holograms that were recorded starting in the nematic phase displayed much higher diffraction efficiencies, with the highest values of η at recording temperatures ca. 10 °C below the isotropic phase transition temperatures of the monomer mixtures. Thirteen orders of diffraction could be observed occasionally. Further decreasing the recording temperature decreased η gradually.

The maximum value of η amounted to 16%. For the holographic gratings in our experiments, which fall in the so-called thin regime, a theoretical maximum diffraction efficiency of ca. 35% is possible.[17] Our values, therefore, are quite good, since no special effort was taken to optimize the results, e.g., by changing the grating constant or the refractive indexes. The reason the diffraction efficiency displays a maximum just below the phase transition temperature of the monomer mixture will be clarified below.

Surface Structure. Since differences in polymer densities between the illuminated and the shadowed areas in the lithographic films were assumed from the observed thickness variations (vide supra), it may be

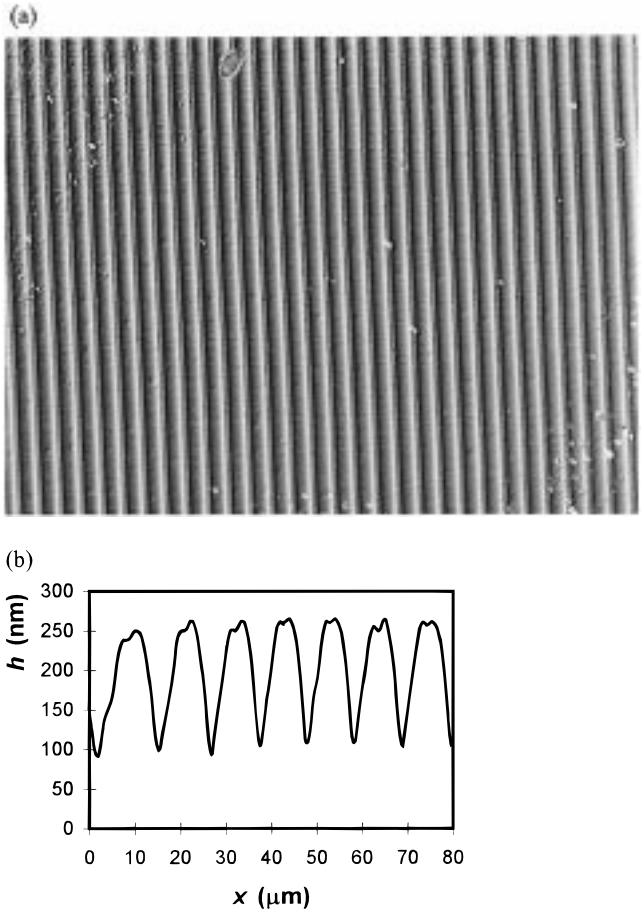

Figure 8. Surface structure of a hologram (30 mol % **MA**, T_{rec} = 70 °C): (a) optical micrograph obtained by sideway illumination; (b) AFM surface profile.

anticipated that a similar phenomenon can arise in the holograms. We therefore studied some of the films with optical and atomic force microscopy (AFM). Figure 8 shows an optical micrograph obtained by sideway illumination and the corresponding AFM surface profile, of a hologram containing 30 mol % **MA** recorded at 70 °C. A very uniform grating structure is visible, with a distinct surface profile, which arose from polymer relaxation after removal of the cover glass plate. The surface amplitude amounted to ca. 145 nm, which is comparable with the amplitude observed for the lithographic films. The surface profiles varied a lot without strong correlation to the polymerization temperature or the **MA**/**DA** ratio. Therefore, the differences in diffraction efficiency of the holograms are not caused by any possible differences in polymer densities.

Polarizing Microscopy. All holograms were examined with the polarizing microscope. Like in the case of the lithographic films, two types of results were obtained. The holograms that were recorded in the isotropic phase showed polymerization-induced orientation effects in the areas with maximum light intensity, similar to what was observed in the lithographic experiments. Also the values of the birefringence were comparable.

The holograms that were recorded in the macroscopically oriented nematic phase displayed interesting features. The birefringence of the illuminated areas amounted to ca. 0.12, which slightly increased with decreasing polymerization temperature. These illuminated areas, however, were alternated with small

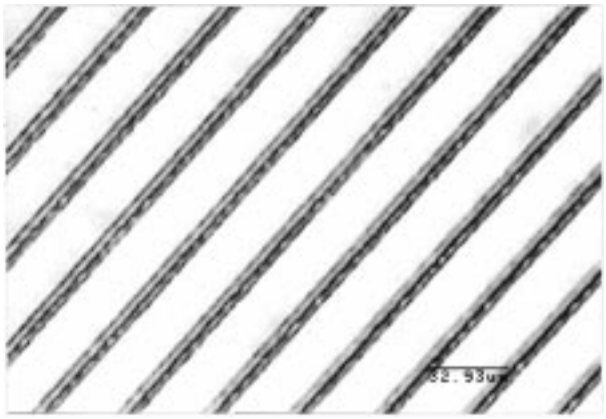

Figure 9. Polarizing micrograph (crossed polarizers) of a hologram containing 30 mol % **MA** recorded at 75 °C (bar = 13 μm).

isotropic lines (Figure 9). Obviously, a transition from the nematic to the isotropic phase must have occurred in the dark regions during the holographic recording. The most simple explanation for this phase transition is that it is due to an increase of the amount of isotropic monoacrylate **MA** in the dark zones, which is in line with our previous expectations (see Introduction). This phenomenon can also explain why the maximum diffraction efficiency was found just below the phase transition temperature: the local phase transition can be most effectively reached at these temperatures, since it would require only a minor increase in the concentration of **MA**. The next section will give strong evidence that such a local compositional change indeed takes place.

Theoretical Models and Verification with Fluorescent Labeling. *Calculations*. Monomer diffusion during holographic and lithographic recording with photopolymers have been simulated previously[6,26,27] but have not dealt with mixtures of monomers with different reactivities. We used therefore a simple method of calculating the diffusion process during nonuniform illumination of a mixture of monoacrylate **MA** and diacrylate **DA**, which is described in the Experimental Section. First, we calculated the changes in the distribution of both components when a sample is partitioned in two positions, one exposed to zero light intensity (I_1 = 0 in eqs 2a−d), and one with maximum light intensity (I_2 = 1). Figure 10a shows for a mixture containing 30 mol % **MA** the calculated sum of free monomer and polymerized acrylate, *f*, in each position during the course of the photopolymerization reaction, for **MA** as well as for **DA**. It is obvious from this figure that the amount of monoacrylate decreases in the illuminated position and increases in the dark position, whereas the opposite effect is calculated for the diacrylate. When 100% conversion is approached in the illuminated position, the difference in monoacrylate content between the light and dark position amounts to 0.183. This calculation was also performed for other starting values of the molar ratio **MA**/**DA**. The final composition difference that is reached for different starting ratios is plotted in Figure 10b. It can be seen that the maximum composition difference is reached when the mixture initially contains a 1:1 molar ratio of **MA** and **DA**.

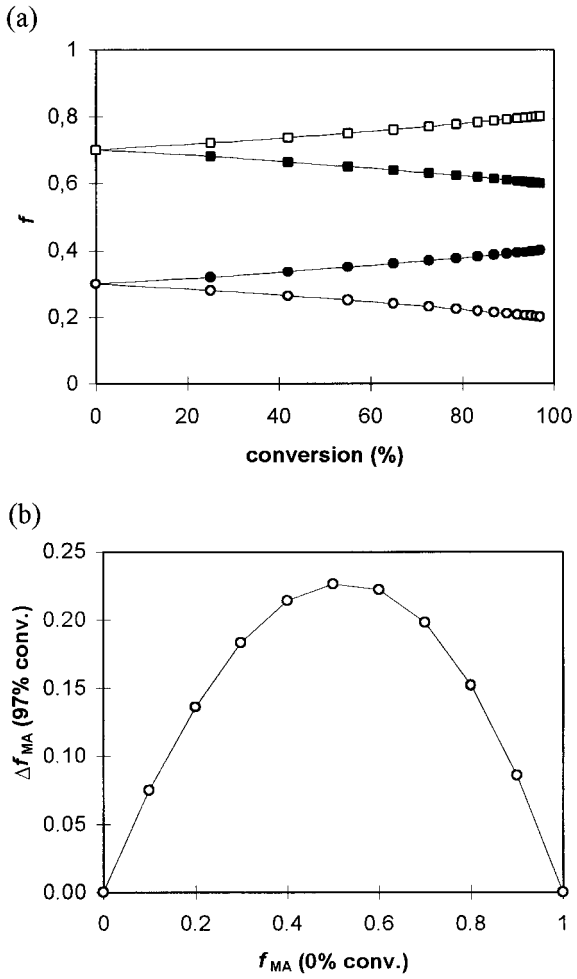

Figure 10. (a) Simulation of the diffusion process of a mixture containing a molar ratio of **MA**/**DA** = 3:7, partitioned in one illuminated zone and one dark zone: calculated sum of molar fractions of monomeric and polymerized acrylates (f_{MA} = [mMA] + [pMA], f_{DA} = [mDA] + [pDA]) as a function of the conversion: (○) f_{MA} in illuminated position; (●) f_{MA} in dark position; (□) f_{DA} in illuminated position; (■) f_{DA} in dark position; (b) difference in monoacrylate molar fractions f_{MA} between illuminated and dark position at 97% conversion as a function of the starting ratio of **MA**/**DA**.

We also applied in our calculations a sinusoidal intensity profile covering 19 positions in each period. Figure 11 shows for each position how the monoacrylate fraction (sum of monomeric and polymerized monoacrylate) changes during the course of the reaction, starting with a 1:1 mixture of **MA** and **DA**. In the positions with minimum light intensities a continuous increase of monoacrylate content is calculated, whereas in positions with maximum intensities the amount of **MA** rapidly decreases in the beginning of the reaction, until a constant level is reached when the conversion approaches to 100%. From the calculated changes of the composition profile during the reaction two important conclusions can be derived: (i) exposure of a mixture of two acrylates, which differ in reactivity, to a sinusoidal intensity profile may lead to a spatial modulation of the composition; (ii) the final distribution of the acrylates deviates from the sinusoidal intensity profile: the peaks are smaller than the valleys (see Figure 11). To verify the calculated composition modulation, we carried out fluorescence microscopy experiments.

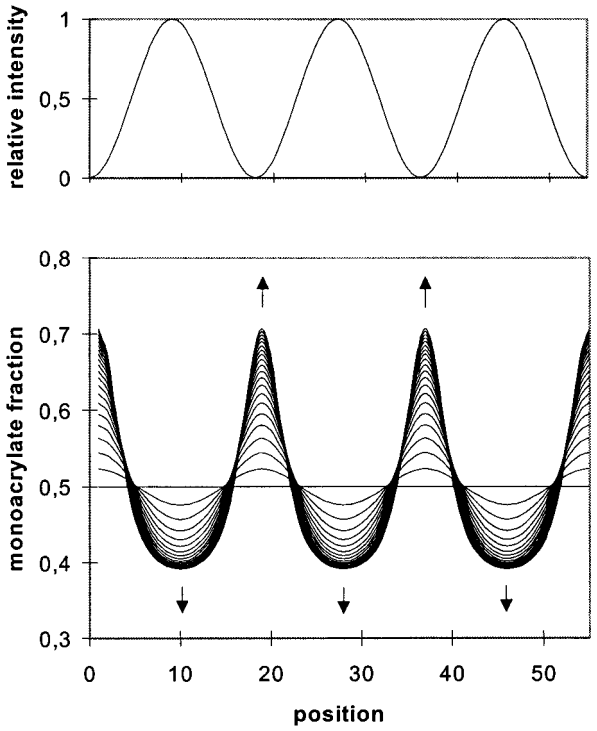

Figure 11. Simulation of the diffusion process when a mixture containing a molar ratio of **MA**/**DA** = 1:1 is illuminated with the sinusoidal intensity profile shown in the upper graph. The development of a compositional profile with intervals of 10 calculation cycli between each curve is shown in the lower graph.

Fluorescent Labeling of Polymer Films. Fluorescence microscopy is a convenient method to analyze the morphology and composition of polymers and composites. Fluorescent polymers can be obtained by copolymerization with a monomer containing a fluorescent dye[28] or by covalent coupling of a reactive dye to the polymer chain in solution.[29] Surface modification of polymer films with fluorescent labels has also been reported.[30] Besides conventional microscopy, scanning near-field optical microscopy techniques have been applied to visualize the distribution of fluorescent probes in polymer materials.[31,32]

We used the possibility of surface modification of the hydroxy groups in our monoacrylate **MA** units, combined with conventional fluorescence microscopy to visualize the composition of our polymer films. We chose a fluorescent probe that is highly reactive with alcohols and can be excited at wavelengths outside the absorption band of the photoinitiator that was still present in the polymer. 9-Anthroylnitrile (**9-AN**) is a dye molecule that meets these requirements (absorption maximum is at ca. 370 nm). Moreover, this compound is soluble is acetonitrile, one of the few solvents that appeared not to swell our polymer films.

(28) Li, L.; Sosnowski, S.; Chaffey, C. E.; Balke, S. T.; Winnik, M. A. *Langmuir* **1994**, *10*, 2495.
(29) Billingham, N. C.; Calvert, P. D.; Uzuner, A. *Polymer* **1990**, *31*, 258.
(30) Ivanov, V. B.; Behnisch, J.; Holländer, A.; Mehdorn, F.; Zimmermann, H. *Surf. Interface Anal.* **1996**, *24*, 257 and references therein.
(31) Moers, M. H. P.; Gaub, H. E.; van Hulst, N. F. *Langmuir* **1994**, *10*, 2774.
(32) Rücker, M.; Vanoppen, P.; De Schryver, F. C.; Ter Horst, J. J.; Hotta, J.; Masuhara, H. *Macromolecules* **1995**, *28*, 7530.

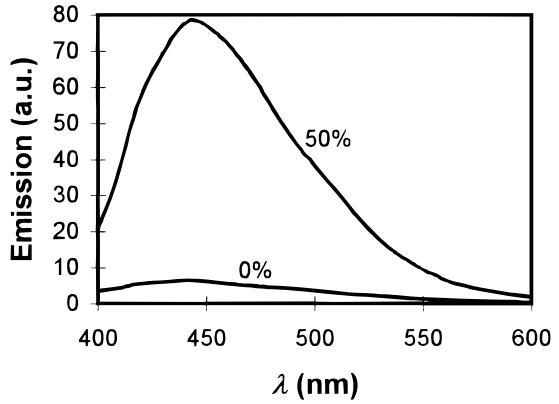

Figure 12. Fluorescence emission spectra of homogeneous polymer films containing 0 mol % **MA** and 50 mol % **MA**, labeled with **9-AN**.

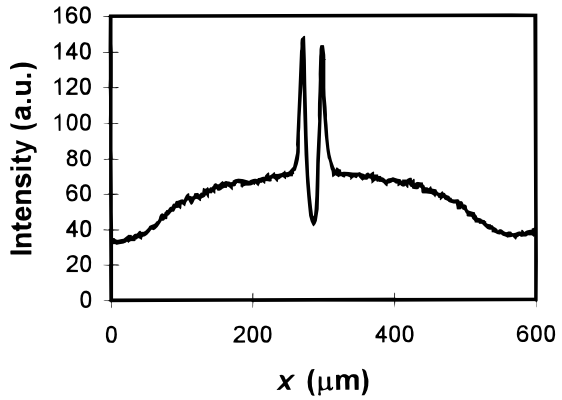

Figure 13. Intensity profile of a fluorescence micrograph obtained from a lithographically illuminated and subsequently labeled film (shadow area of a 1000 μm grating in a film containing 30 mol % **MA** polymerized at 50 °C).

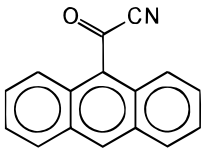

9-AN

To determine whether the probe molecules could selectively label the polymerized **MA** units, we treated two uniformly polymerized films with **9-AN**, one film containing pure **DA** polymer, and one containing 50 mol % **MA**. We recorded the emission spectra of both labeled films, which are displayed in Figure 12. It is obvious from the spectra that the film containing **MA** is highly fluorescent. The **DA** film has a low emission intensity which is probably due to some residual unreacted probe molecules. From this result we expected that it would be possible to visualize local differences in **MA** content in the lithographic and holographic films by reacting **9-AN** with the alcohol groups of **MA** present at the surface of the samples.

Fluorescence Microscopy. The lithographically illuminated films were treated with **9-AN** and inspected with a fluorescence microscope. The films mostly showed uniform fluorescence. Sometimes, however, faint-line patterns could be seen at sites with small grating constants, and more distinct patterns could be discerned at the 200 and 1000 μm gratings. Figure 13 shows the fluorescence intensity profile measured on the largest grating in one sample. It reveals a ca. 500 μm broad fluorescent band at the masked zone of the grating. The two peaks in the middle of the band arise from the two walls of one of the empty channels that had been observed in previous experiments (vide supra). Because we were looking from a direction parallel to the plane of these walls, which are covered by dye molecules, they are seen as two high-intensity lines. In summary, it is obvious from this result that the amount of labeled monoacrylate in the shadow zones is larger than in the surrounding illuminated zones. Apparently, the shadow zone had been enriched with monoacrylate, which corroborates our idea that the monoacrylate preferably diffuses to the shadow areas and the diacrylate to the illuminated areas.

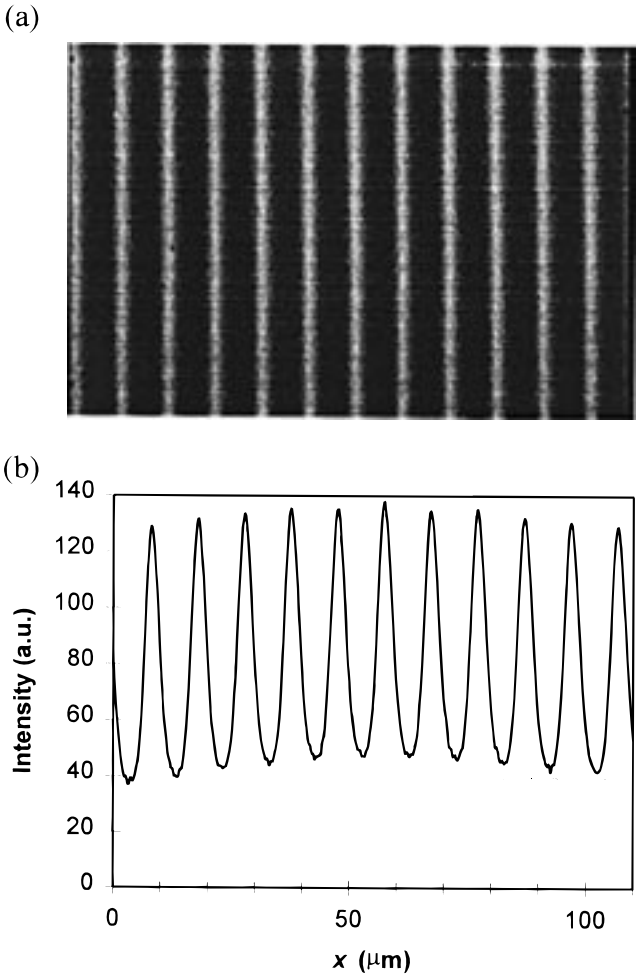

Figure 14. Fluorescence pattern of a hologram (30 mol % **MA**, recorded at $T = 70$ °C, $I = 0.12$ mW cm^{-2}): (a) fluorescence micrograph; (b) intensity profile.

The same labeling experiments were carried out with our holographically illuminated films. Every sample displayed very clear fluorescent lines with a periodicity corresponding to the grating constant of 10 μm. Figure 14a shows an example of a fluorescence micrograph, and Figure 14b the corresponding intensity profile of the hologram.

We assume that the measured fluorescence intensity is proportional to the amount of monoacrylate present at the surface. The proportionality constant probably is unequal for different samples, because of possible differences in conditions (e.g., temperature, concentra-

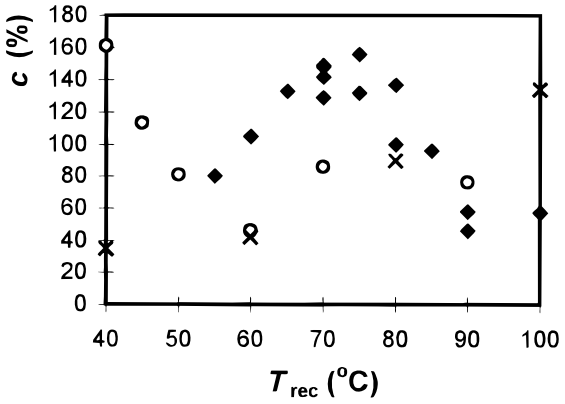

Figure 15. Fluorescence contrasts of the holograms as a function of the recording temperature for polymerized samples containing 30 (▼), 50 (○), and 70 (×) mol % **MA**.

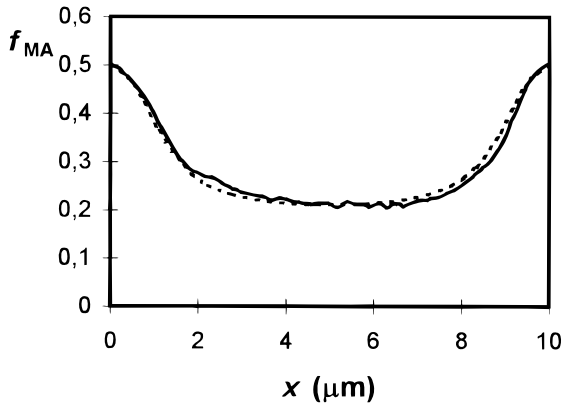

Figure 16. Broken line: calculated compositional profile after 250 polymerization/diffusion cycli when a sinusoidal intensity profile was applied to a film containing 30 mol % **MA** (see Figure 4b for comparison). Solid line: one period of the normalized fluorescence intensity profile of Figure 14b (f_{MA} = 0.004 23 × intensity).

tion, reaction time) during the labeling process. To be able to compare the results of different samples, we eliminated therefore the proportionality constant by calculating the contrast c in each sample according to the equation

$$c = (I_{max} - I_{min})/I_{min} \quad (10)$$

in which I_{max} and I_{min} are the maximum and minimum fluorescence intensities of the grating periods. A large fluorescence contrast c means that an efficient opposite diffusion of monoacrylate and diacrylate has taken place.

The contrasts for holographic samples of three different compositions polymerized at various temperatures are plotted in Figure 15. First, we will discuss the data points obtained from samples containing 70 mol % **MA**, which were all polymerized in the isotropic phase. The fluorescence contrast of the sample polymerized at 60 °C is similar to that of the one polymerized at 40 °C, probably because the higher diffusion rate at 60 °C is counteracted by the higher polymerization rate. Further increase of the polymerization temperature results in increasing contrasts, which is explained by the fact that above 60 °C the polymerization rate decreases.

Also in the case of the samples containing 30 mol % **MA** an increasing contrast with increasing temperature is observed when the holographic recording is carried out in the nematic phase below 80 °C (Figure 15). However, when the recording temperature was close to and above the phase transition of the monomeric mixture, a substantial lower fluorescence contrast was measured. Apparently, the diffusion rate in the isotropic phase is lower than in the nematic phase. This may be due to the fact that in the latter phase the diffusion direction is parallel to the long axes of the macroscopically oriented molecules, which is more favorable. This hypothesis was proven by an experiment in which the orientation of the molecules was made parallel instead of perpendicular to the direction of the grating lines. The fluorescence contrast was decreased from a value of 1.48 to 0.61. Also, the contrast appeared to be dependent on the laser power used to record the holograms. A higher light intensity resulted in a lower fluorescence contrast and vice versa, as can be expected from the intensity dependence of the polymerization rate.

At this point we are able to relate the performance, i.e., the diffraction efficiency, of the holographic gratings to the diffusion process. In the isotropic phase, the temperature dependence of the compositional modulations as observed by fluorescence microscopy (Figure 15) is not related to the diffraction efficiency (Figure 7b). This is understandable because the isotropic refractive index of the monomer mixture appeared to be only weakly dependent on the composition of the mixture (for 30 mol % **MA** and 60 mol % **MA** at 85 °C n_i equals 1.532 and 1.523, respectively). The large diffraction efficiency in the nematic phase is mainly the result of the alternation of oriented and isotropic lines, realized by the opposite diffusion of the two monomeric components which is enhanced by the proper alignment of the long axes of the molecules in the diffusion direction. The extraordinary refractive index of the oriented areas is considerably larger than the isotropic refractive index (e.g., for 30 mol % **MA** n_e = 1.582 at 75 °C, for 60 mol % **MA** n_i = 1.526 at the same temperature). This increased refractive index difference explains the increased diffraction efficiency of the grating. As can be expected from the birefringence of the oriented areas, the diffraction appeared to depend on the polarization of the incoming light, but this has not yet been investigated systematically.

Comparison with Theory. The measured fluorescence intensity profiles were fitted to the calculated composition profiles by multiplication of the measured values with a single interconversion factor and by application of a certain number of calculated polymerization/diffusion cycli, respectively.

The measured fluorescence intensity profile of a hologram containing 30 mol % **MA** recorded at 70 °C with a low laser power, multiplied by a factor of 4.23 × 10^{-3}, is displayed in Figure 16, together with the calculated compositional profile that was obtained after 250 calculation cycli. The similarity between the two curves is remarkable. However, it must be mentioned that the correspondence between experiment and theory was less for holograms that displayed lower diffraction efficiencies recorded at other temperatures and with higher laser intensities. Nevertheless, the experimental and theoretical results allow one to make some important conclusions:

(i) The experimental conditions for recording the hologram that displayed the highest diffraction efficiency apparently were such that complete diffusion could take place (the calculations were based on complete diffusion).

(ii) The opposite diffusion process which takes place in the samples can reasonably be described by the used model. A better match with nonequilibrium conditions is expected when the diffusion laws are included.

(iii) The assumed ratio of two between the polymerization rates of the monoacrylate and the diacrylate seems to be based on reality.

(iv) Fluorescent labeling is a very convenient and reliable method to study the composition of our polymer films.

In summary, the data presented in this paper provide good evidence that nonuniform polymerization of a mixture of two monomers with different photoreactivities leads to opposite diffusion of the monomers. This process results in local changes of the composition, which may lead to changes of properties. In our case we used a nematic diacrylate and an isotropic monoacrylate to accomplish local phase transitions. The use of holography appears to be superior to lithography when making uniform and well-defined grating structures with an alternation of oriented and isotropic lines. Good diffraction efficiencies are obtained. We expect, however, that the results can be further improved by using smaller gratings and a better tuning of the refractive indexes of the two monomers. Current research aims at such objectives.

Acknowledgment. This research was financially supported by the Foundation of Technical Sciences (STW). We thank Dr. J. Lub for assistance in the syntheses of the compounds, Dr. H. Boots for fruitful discussions, and Mrs. C. de Witz for technical support.

CM970305L